Cyber-Physical Systems

ISSN: 2333-5777 (Print) 2333-5785 (Online) Journal homepage: https://www.tandfonline.com/loi/tcyb20

Non-linear optimal control for four-wheel omnidirectional mobile robots

G. Rigatos, K. Busawon, M. Abbaszadeh & P. Wira

CYBER-PHYSICAL SYSTEMS
https://doi.org/10.1080/23335777.2020.1716269

Taylor & Francis
Taylor & Francis Group

Check for updates

Non-linear optimal control for four-wheel omnidirectional mobile robots

G. Rigatos [a], K. Busawon [b], M. Abbaszadeh [c] and P. Wira [d]

[a]Unit of Industrial Autom, Industrial Systems Institute, Patras, Greece; [b]Nonlinear Control Group, University of Northumbria Newcastle, Newcastle, UK; [c]GE Global Research, General Electric, NY, USA; [d]IRIMAS, IRIMAS University D' Haute Alsace, Mulhouse, France

ABSTRACT
The article proposes a non-linear optimal control approach for four-wheel omnidirectional mobile robots. The method has been successfully tested so-far on the control problem of several types of autonomous ground vehicles and the present article shows that it can also provide the only optimal solution to the control problem of four-wheel omnidirectional robotic vehicles. To implement this control scheme, the state-space model of the robotic vehicle undergoes first approximate linearisation around a temporary operating point, through first-order Taylor series expansion and through the computation of the associated Jacobian matrices. To select the feedback gains of the H-infinity controller an algebraic Riccati equation is repetitively solved at each time-step of the control method. The global stability properties of the control loop are proven through Lyapunov analysis. Finally, to implement state estimation-based feedback control, the H-infinity Kalman Filter is used as a robust state estimator.

ARTICLE HISTORY
Received 30 August 2019
Accepted 31 December 2019

KEYWORDS
Omnidirectional mobile robots; non-linear optimal control; H-infinity control; algebraic Riccati equation; Lyapunov stability analysis; global asymptotic stability

1 Introduction

Four-wheel omnidirectional vehicles allow for agile manoeuvring and perform well in all-terrain motion [1–5]. They can find applications in transportation and defence tasks [6–9]. The control of four-wheel omnidirectional robots exhibits difficulties [10–13]. This is because of the non-linear and multivariable structure of the associated state-space model and because of overactuation [14–17]. Although one could consider that through linearisation approaches it becomes possible to solve the trajectory tracking control problem for such a type of robots, the implementation of control under optimality criteria, that is minimum energy consumption, remains an open problem [18–21].

Non-linear control of omnidirectional four-wheel mobile robots is an open topic which is still attracting much research interest [22–25]. Non-linear control

CONTACT G. Rigatos grigat@ieee.org Unit of Industrial Automation, Industrial Systems Institute, 26504, Rion Patras, Greece.

of proven global stability is a challenging objective which can improve the performance of omnidirectional four-wheel mobile robots, in terms of precise path tracking and operational capacity [18,26–28]. One can note that, in the model of the four-wheel omnidirectional robot, popular approaches for solving the optimal control problem in industrial systems, such as MPC (Model Predictive Control) and NMPC (Nonlinear Model Predictive Control) may be inefficient. This is because MPC is primarily addressed to linear systems and under the non-linear dynamics of this robotic vehicle the MPC control loop is likely to become unstable. Besides, the iterative search for an optimum performed by the NMPC is not of assured convergence either and can be dependent on initialisation. As a result NMPC is not of proven global stability and cannot ensure the reliable functioning of the control loop of the omnidirectional four-wheel robot. Besides, taking into account that the dynamic model of this robotic vehicle is not in a multivariable canonical form, the application of sliding mode control is not straightforward and is inhibited by the need to define a sliding surface with the use of intuition and in an ad-hoc manner. Finally, the use of PID control for the non-linear multivariable model of the four-wheel omnidirectional robot is by far unacceptable, since it lacks global stability and may function only around local operating points.

In the present article, a new non-linear optimal (H-infinity) control method is developed for four-wheel omnidirectional robotic vehicles [29,30]. First, approximate linearisation of the state-space model of the robot is carried out around a temporary operating point which is recomputed at each iteration of the control algorithm. The linearisation point is defined by the present value of the system's state vector and by the last sampled value of the control inputs vector. The linearisation takes place through first-order Taylor series expansion and through the computation of the associated Jacobian matrices [31–33]. The modelling error which is due to the truncation of higher-order terms in the Taylor series is considered to be a perturbation which is finally compensated by the robustness of the control method.

The proposed H-infinity controller implements a solution to the optimal control problem of the omnidirectional robotic vehicle under model uncertainty and external perturbations. Actually, the H-infinity control method represents a min-max differential game in which the controller tries to minimise a quadratic cost function of the state vector's tracking error, whereas the model uncertainty terms and external perturbations try to maximize this cost function. To compute the feedback gains of a stabilising H-infinity controller an algebraic Riccati equation has to be repetitively solved at each time-step of the control method [34–36]. The stability properties of the control scheme are proven through Lyapunov analysis. First, it is demonstrated that the control loop satisfies the H-infinity tracking performance criterion, which signifies elevated robustness against modelling errors and exogenous disturbances [37,38]. Moreover, it is proven that under moderate conditions the control loop is globally asymptotically stable. Finally, to implement H-infinity feedback control without the need to measure the entire state vector of the mobile robot, the H-infinity Kalman Filter is proposed as a robust state estimator [39,40].

The structure of the article is as follows: in Section 2 the dynamic model of the four-wheel omnidirectional mobile robot is analysed and the related state-space model is given. In Section 3 the state-space model of the mobile robot undergoes approximate linearisation through the computation of the associated Jacobian matrices. Besides an H-infinity controller is formulated for the linearised model of the robotic vehicle. In Section 4 Lyapunov stability analysis is carried out to prove the global stability properties of the control scheme. In Section 5 the H-infinity Kalman Filter is introduced as a robust state estimator which allows for implementation of feedback control through the measurement of a small number of state vector elements of the robot. In Section 6 the tracking performance of the control method is tested through simulation experiments. Finally, in Section 7 concluding remarks are stated.

2 Dynamic model of the four-wheel omnidirectional robot

The diagram of the four-wheel omnidirectional robot together with the inertial and body-fixed reference frames is shown in Figure 1. One defines as (x, y) the coordinates of the robot's centre of gravity and as θ its orientation angle, that is the angle that is defined by its longitudinal axis and the horizontal axis of the inertial reference frame. Moreover, the velocity of the vehicle along the

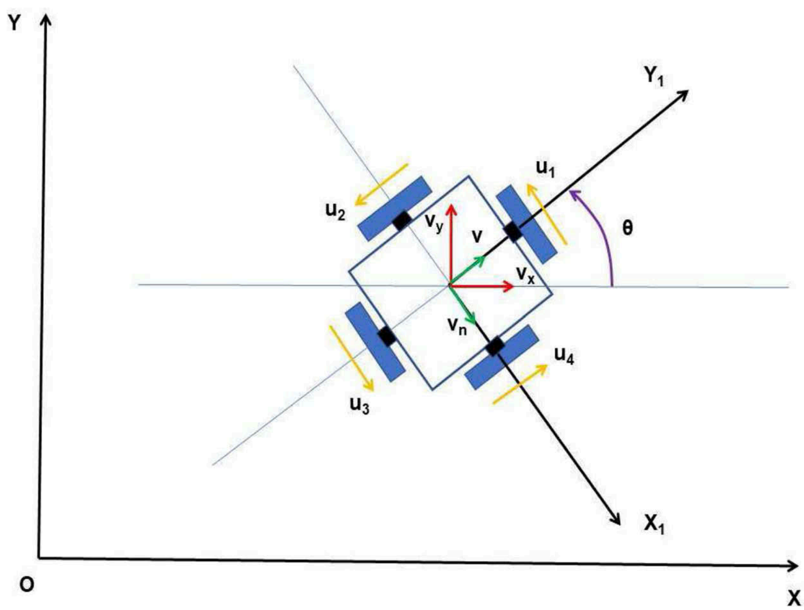

Figure 1. Diagram of the four-wheel omnidirectional robot together with reference axes.

horizontal axis of the inertial frame is defined as v_x while its velocity along the vertical axis is defined as v_y and finally its turn (yaw) speed is defined as ω. The torques which are developed by the motors of the vehicle and which cause the rotation of its wheels are denoted as u_1, u_2, u_3 and u_4. Then, the dynamics of the four-wheel omnidirectional model is shown to be defined by the following set of differential Equations [6] and [10]. Actually, about the vehicle's velocity in the inertial reference frame one has

$$\frac{dx}{dt} = v_x \tag{1}$$

$$\frac{dy}{dt} = v_y \tag{2}$$

$$\frac{d\theta}{dt} = \omega \tag{3}$$

The vector of linear velocities in the inertial coordinates system is $[\dot{x}, \dot{y}]^T = [v_x, v_y]^T$, while the vector of linear velocities in the body-fixed coordinates is $[v, v_n]^T$. Between the two aforementioned velocity vectors the following relation holds

$$\begin{pmatrix} v_x \\ v_y \end{pmatrix} = \begin{pmatrix} cos(\theta) & -sin(\theta) \\ sin(\theta) & cos(\theta) \end{pmatrix} \begin{pmatrix} v \\ v_n \end{pmatrix} \tag{4}$$

which is also written in the following form:

$$\begin{array}{c} v_x = vcos(\theta) - v_n sin(\theta) \\ v_y = vsin(\theta) + v_n cos(\theta) \end{array} \tag{5}$$

Assume next the Newtonian laws of motion in the body-fixed reference frame. It holds

$$\begin{array}{c} M\dot{v} = \sum_{i=1}^{N} F_{x_i} \Rightarrow M\dot{v} = F_v - F_{B_v} - F_{C_v} \\ M\dot{v}_n = \sum_{i=1}^{N} F_{y_i} \Rightarrow M\dot{v}_n = F_{v_n} - F_{B_{v_n}} - F_{C_{v_n}]} \\ M\dot{\omega} = \sum_{i=1}^{N} T \Rightarrow M\dot{\omega} = T - T_{B_w} - T_{C_w} \end{array} \tag{6}$$

In the previous relation one has that F_{B_v}, $F_{B_{v_n}}$ and T_{B_w} are viscous frictions and torques which are proportional to the linear and the rotational velocity of the vehicle, respectively. Moreover, one has that T_{C_v}, $T_{C_{v_n}}$ and T_{C_w} are Coulomb frictions and torques which depend on the sign of the linear and angular velocities of the vehicle, respectively. Thus, it holds

$$\begin{array}{cc} F_{B_v} = B_v v & F_{C_v} = C_v \frac{v}{|v|} \\ F_{B_{v_n}} = B_{v_n} v_n & F_{C_{v_n}} = C_{v_n} \frac{v}{|v_n|} \\ T_{B_w} = B_w \omega & T_{C_w} = C_w \frac{\omega}{|\omega|} \end{array} \tag{7}$$

About the forces and torques which are exerted on the robotic vehicle by its motors it holds that

$$\begin{array}{c} F_v = F_4 - F_2 \\ F_{v_n} = F_1 - F_3 \\ T_z = (F_1 + F_2 + F_3 + F_4)d \end{array} \tag{8}$$

where d is the distance of each wheel from the vehicle's centre of gravity. Besides for each wheel of the vehicle, the traction force is

$$\begin{array}{c} f(t) = \frac{T_w(t)}{r} \\ T_w(t) = lK_t i_a \end{array} \tag{9}$$

where $T_w(t)$ is the wheel's torque which is related to the motor's torque $T_m(t) = K_t i_a$ through the transmission ratio l, that is $T_w = lT_m(t)$. It holds that K_t is the motor's torque constant and i_a is the motor's armature current. About the electrical dynamics of the motor one has

$$\begin{array}{c} V = L_a \frac{dI_a}{dt} + R_a I_a + K_w \omega_m \\ T_m = K_t i_a \end{array} \tag{10}$$

with $K_w \omega_m$ to stand for the electromagnetic force which is proportional to the motor's turn speed. From Equations (6) to (9) one obtains that

$$\begin{array}{c} M\dot{v} = (f_4 - f_2) - B_v v - C_v \frac{v}{|v|} \\ M\dot{v}_n = (f_1 - f_3) - B_{v_n} v_n - C_{v_n} \frac{v_n}{|v_n|} \\ J\dot{\omega} = (f_1 + f_2 + f_3 + f_4)d - B_w \omega - C_w \frac{\omega}{|\omega|} \end{array} \tag{11}$$

or equivalently

$$\begin{array}{c} \dot{v} = \frac{1}{M} f_4 - \frac{1}{M} f_2 - \frac{B_v}{M} v - \frac{C_v}{M} sign(v) \\ \dot{v}_n = \frac{1}{M} f_1 - \frac{1}{M} f_3 - \frac{B_{vn}}{M} v_n - \frac{C_{vn}}{M} sign(v_n) \\ \dot{\omega} = \frac{d}{J} f_1 + \frac{d}{J} f_2 + \frac{d}{J} f_3 + \frac{d}{J} f_4 - \frac{B_w}{J} \omega - \frac{C_w}{J} sign(\omega) \end{array} \tag{12}$$

where the force f_i $i = 1, \ldots 4$ is given by

$$f_i = \frac{1}{r} T_i \Rightarrow f_i = \frac{1}{r} lK_t^i i_a \Rightarrow f_i = \frac{l}{r} T_m^i \tag{13}$$

By substituting the previous equation into Equation (12) one gets

$$\begin{array}{c} \dot{v} = \frac{1}{M}\frac{l}{r} T_m^4 - \frac{1}{M}\frac{l}{r} T_m^2 - \frac{B_v}{M} v - \frac{C_v}{M} sign(v) \\ \dot{v}_n = \frac{1}{M}\frac{l}{r} T_m^1 - \frac{1}{M}\frac{l}{r} T_m^3 - \frac{B_{vn}}{M} v_n - \frac{C_{vn}}{M} sign(v_n) \\ \dot{\omega} = \frac{d}{J}\frac{l}{r} T_m^1 + \frac{d}{J}\frac{l}{r} T_m^2 + \frac{d}{J}\frac{l}{r} T_m^3 + \frac{d}{J}\frac{l}{r} T_m^4 - \frac{B_w}{J} \omega - \frac{C_w}{J} sign(\omega) \end{array} \tag{14}$$

Next, using Equation (4) one obtains

$$\begin{array}{c} v = cos(\theta)\dot{x} + sin(\theta)\dot{y} \\ v_n = -sin(\theta)\dot{x} + cos(\theta)\dot{y} \end{array} \tag{15}$$

By differentiating $\dot{x}$, $\dot{y}$ and $\dot{\theta}$ given in Equations (1)–(3) one finds the following description of the dynamics of the omnidirectional mobile robot:

$$\begin{array}{c}\ddot{x}=\dot{v}cos(\theta)-vsin(\theta)\dot{\theta}-\dot{v}_n sin(\theta)-v_n cos(\theta)\dot{\theta} \\ \ddot{y}=\dot{v}sin(\theta)+vcos(\theta)\dot{\theta}+\dot{v}_n cos(\theta)-v_n sin(\theta)\dot{\theta} \\ \ddot{\theta}=\dot{\omega}\end{array} \tag{16}$$

By substituting Equation (14) into the first row of Equation (16) one obtains:

$$\begin{array}{c}\ddot{x}=\{\frac{l}{Mr}T_m^4-\frac{l}{Mr}T_m^2-\frac{B_v}{M}v-\frac{C_v}{M}sign(v)\}cos(\theta)-vsin(\theta)\dot{\theta} \\ -\left\{\frac{l}{Mr}T_m^1-\frac{l}{Mr}T_m^2-\frac{B_{vn}}{M}v_n-\frac{C_{vn}}{M}sign(v_m)\right\}sin(\theta)-v_n cos(\theta)\dot{\theta}\end{array} \tag{17}$$

Next, by substituting in the previous equation v and v_n from Equation (15) and after intermediate operations one gets

$$\begin{array}{l}\ddot{x}=\left[\frac{B_{vn}}{M}sin^2(\theta)-\frac{B_v}{M}cos^2(\theta)\right]\dot{x}+\left[-\left(\frac{B_v}{M}+\frac{B_{vn}}{M}\right)sin(\theta)cos(\theta)\right]\dot{y}-\dot{y}\dot{\theta}- \\ -\frac{C_v}{M}sign(cos(\theta)\dot{x}+sin(\theta)\dot{y})cos(\theta)-\frac{C_{vn}}{M}sign(-sin(\theta)\dot{x}+cos(\theta)\dot{y})sin(\theta)- \\ -\frac{l}{Mr}sin(\theta)T_m^1-\frac{l}{Mr}cos(\theta)T_m^2-\frac{l}{Mr}sin(\theta)T_m^3+\frac{l}{Mr}cos(\theta)T_m^4\end{array} \tag{18}$$

By substituting Equation (14) into the second row of Equation (16) one obtains:

$$\begin{array}{l}\ddot{y}=\{\frac{l}{Mr}T_m^4-\frac{l}{Mr}T_m^2-\frac{B_v}{M}v-\frac{C_v}{M}sign(v)\}sin(\theta)+(cos(\theta)\dot{x}+sin(\theta)\dot{y})cos(\theta)\dot{\theta}+ \\ +\left\{\frac{l}{Mr}T_m^1-\frac{l}{Mr}T_m^3-\frac{B_{vn}}{M}v_n-\frac{C_{vn}}{M}sign(v_n)\right\}cos(\theta)-(-sin(\theta)\dot{x}+cos(\theta)\dot{y})sin(\theta)\dot{\theta}\end{array} \tag{19}$$

Next, by substituting in the previous equation v and v_n from Equation (15) and after intermediate operations one gets

$$\begin{array}{l}\ddot{y}=\left[\left(B_{\frac{vn}{M}}-\frac{B_v}{M}\right)sin(\theta)cos(\theta)\right]\dot{x}+\left[-\frac{B_v}{M}sin^2(\theta)-\frac{B_{vn}}{M}cos^2(\theta)\right]\dot{y}+\dot{x}\dot{\theta}- \\ -\frac{C_v}{M}sin(\theta)sign(cos(\theta)\dot{x}+sin(\theta)\dot{y})-\frac{C_{vn}}{M}cos(\theta)sign(-sin(\theta)\dot{x})+cos(\theta)\dot{y}+ \\ \frac{l}{Mr}cos(\theta)T_m^1-\frac{l}{Mr}sin(\theta)T_m^2-\frac{l}{Mr}cos(\theta)T_m^3-\frac{l}{Mr}sin(\theta)T_m^4\end{array} \tag{20}$$

By substituting Equation (14) into the third row of Equation (16) one obtains:

$$\ddot{\theta}=-\frac{B_w}{J}\omega-\frac{C_w}{J}sign(\omega)+\frac{dl}{Jr}T_m^1+\frac{dl}{Jr}T_m^2+\frac{dl}{Jr}T_m^3+\frac{dl}{Jr}T_m^4 \tag{21}$$

Next, by defining the state variables of the omnidirectional mobile robot as $x_1=x$, $x_2=\dot{x}$, $x_3=y$, $x_4=\dot{y}$, $x_5=\theta$ and $x_6=\dot{\theta}$, and the control inputs of the vehicle as $u_1=T_m^1$, $u_2=T_m^2$, $u_3=T_m^3$ and $u_4=T_m^4$, the state-space description of the system becomes

$$\dot{x}_1=x_2 \tag{22}$$

$$\begin{array}{l}\dot{x}_2=\left[\frac{B_{vn}}{M}sin^2(x_5)-\frac{B_v}{M}cos^2(x_5)\right]x_2+\left[-\left(\frac{B_v}{M}+\frac{B_{vn}}{M}\right)sin(x_5)cos(x_5)\right]x_4-x_4x_6- \\ -\frac{C_v}{M}sign(cos(x_5)x_2+sin(x_5)x_4)cos(x_5)-\frac{C_{vn}}{M}sign(-sin(x_5)x_2 \\ +cos(x_5)x_4)sin(x_5)-\frac{l}{Mr}sin(x_5)u_1-\frac{l}{Mr}cos(x_5)u_2 \\ -\frac{l}{Mr}sin(x_5)u_3+\frac{l}{Mr}cos(x_5)u_4\end{array} \tag{23}$$

$$\dot{x}_3 = x_4 \tag{24}$$

$$\dot{x}_4 = \left[\left(B_{\frac{v_n}{M}} - \frac{B_v}{M}\right) sin(x_5) cos(x_5)\right] x_2 + \left[-\frac{B_v}{M} sin^2(x_5) - \frac{B_{v_n}}{M} cos^2(x_5)\right] x_4 + x_2 x_6 - \\ - \frac{C_v}{M} sin(x_5) sign(cos(x_5) x_2 + sin(x_5) x_4) - \frac{C_{v_n}}{M} cos(x_5) sign(-sin(x_5) x_2 \\ + cos(x_5) x_4) + \frac{l}{Mr} cos(x_5) u_1 - \frac{l}{Mr} sin(x_5) u_2 - \frac{l}{Mr} cos(x_5) u_3 - \frac{l}{Mr} sin(x_5) u_4 \tag{25}$$

$$\dot{x}_5 = x_6 \tag{26}$$

$$\dot{x}_6 = \frac{B_w}{J} x_6 - \frac{C_w}{J} sign(x_6) + \frac{dl}{Jr} u_1 + \frac{dl}{Jr} u_2 + \frac{dl}{Jr} u_3 + \frac{dl}{Jr} u_4 \tag{27}$$

The state-space model of the four-wheel omnidirectional robot can be also written in matrix form:

$$\begin{pmatrix} \dot{x}_1 \\ \dot{x}_2 \\ \dot{x}_3 \\ \dot{x}_4 \\ \dot{x}_5 \\ \dot{x}_6 \end{pmatrix} = \begin{pmatrix} f_1(x) \\ f_2(x) \\ f_3(x) \\ f_4(x) \\ f_5(x) \\ f_6(x) \end{pmatrix} + \begin{pmatrix} g_{11}(x) & g_{12}(x) & g_{13}(x) & g_{14}(x) \\ g_{21}(x) & g_{22}(x) & g_{23}(x) & g_{24}(x) \\ g_{31}(x) & g_{32}(x) & g_{33}(x) & g_{34}(x) \\ g_{41}(x) & g_{42}(x) & g_{43}(x) & g_{44}(x) \\ g_{51}(x) & g_{52}(x) & g_{53}(x) & g_{54}(x) \\ g_{61}(x) & g_{62}(x) & g_{63}(x) & g_{64}(x) \end{pmatrix} \begin{pmatrix} u_0 \\ u_1 \\ u_2 \\ u_3 \end{pmatrix} \tag{28}$$

where $f_1(x) = x_2$, $f_2(x) = \left[\frac{B_{v_n}}{M} sin^2(x_5) - \frac{B_v}{M} cos^2(x_5)\right] x_2 + \left[-\left(\frac{B_v}{M} + \frac{B_{v_n}}{M}\right) sin(x_5)\right.$ $\left. cos(x_5)\right] x_4 - x_4 x_6 - \frac{C_v}{M} sign(cos(x_5) x_2 + sin(x_5) x_4) cos(x_5) - \frac{C_{v_n}}{M} sign(-sin(x_5) x_2,$ $+ cos(x_5) x_4) sin(x_5), f_3(x) = x_4 f_4(x) = \left[\left(B_{\frac{v_n}{M}} - \frac{B_v}{M}\right) sin(x_5) cos(x_5)\right] x_2 + \left[-\frac{B_v}{M} sin^2(x_5),\right.$ $\left. -\frac{B_{v_n}}{M} cos^2(x_5)\right] x_4 + x_2 x_6 - \frac{C_v}{M} sin(x_5) sign(cos(x_5) x_2 + sin(x_5) x_4) - \frac{C_{v_n}}{M} cos(x_5) sign$ $(-sin(x_5) x_2 + cos(x_5) x_4), f_5(x) = x_6$, and $f_6(x) = \frac{B_w}{J} x_6 - \frac{C_w}{J} sign(x_6)$.
and $g_{11}(x) = 0$, $g_{12}(x) = 0$, $g_{13}(x) = 0$ and $g_{14}(x) = 0$, $g_{21}(x) = -\frac{l}{Mr} sin(x_5)$, $g_{22}(x) = -\frac{l}{Mr} cos(x_5)$, $g_{23}(x) = -\frac{l}{Mr} sin(x_5)$, $g_{24}(x) = \frac{l}{Mr} cos(x_5)$, $g_{31}(x) = 0$, $g_{32}(x) = 0$, $g_{33}(x) = 0$, $g_{34}(x) = 0$, $g_{41}(x) = \frac{l}{Mr} cos(x_5)$, $g_{42}(x) = -\frac{l}{Mr} sin(x_5)$, $g_{43}(x) = -\frac{l}{Mr} cos(x_5)$, $g_{44}(x) = -\frac{l}{Mr} sin(x_5)$, $g_{51}(x) = 0$, $g_{52}(x) = 0$, $g_{53}(x) = 0$, $g_{54}(x) = 0$ and $g_{61}(x) = \frac{dl}{Jr}$, $g_{62}(x) = \frac{dl}{Jr}$, $g_{63}(x) = \frac{dl}{Jr}$, $g_{64}(x) = \frac{dl}{Jr}$.

The measured state variables of the robot are taken to be the Cartesian coordinates of its centre of gravity, that is $x_1 = x$ and $x_3 = y$, as well as the heading angle of the vehicle that is $x_5 = \theta$. Thus, the measurement equation of the system is

$$\begin{pmatrix} y_1 \\ y_2 \\ y_3 \end{pmatrix} = \begin{pmatrix} 1 & 0 & 0 & 0 & 0 & 0 \\ 0 & 0 & 1 & 0 & 0 & 0 \\ 0 & 0 & 0 & 0 & 1 & 0 \end{pmatrix} \begin{pmatrix} x_1 \\ x_2 \\ x_3 \\ x_4 \\ x_5 \\ x_6 \end{pmatrix} \tag{29}$$

Thus, finally, the state-space model of the four-wheel omnidirectional mobile robot can be written in the following concise form:

$$\dot{x} = f(x) + g(x)u \tag{30}$$

where $x \in R^{6\times1}$, $f(x) \in R^{6\times1}$, $g(x) \in R^{6\times3}$ and $u \in R^{3\times1}$.

3 Approximate linearisation of the state-space model of the omnidirectional robot

3.1 Approximate linearisation of the state-space model

The state-space model of the omnidirectional mobile robot undergoes approximate linearisation around the temporary operating point (x^*, u^*), where x^* is the present value of the system's state vector and u^* is the last sampled value of the control inputs vector. The linearisation point is updated at each time-step of the control algorithm. The linearisation relies on Taylor series expansion and on the computation of the associated Jacobian matrices. The approximately linearised model is rewritten as:

$$\dot{x} = Ax + Bu + \tilde{d} \tag{31}$$

where $\tilde{d}$ is the modelling error due to truncation of higher-order terms in the Taylor series expansion and due to external perturbations. For the control inputs gain matrix $g(x)$ its decomposition per column gives $g(x) = [g_1(x), g_2(x)]$, $g_3(x), g_4(x)]^T$. Matrices A and B given in Equation (31) are described by the following Jacobians of the system

$$\begin{aligned} A = \nabla_x f(x)|_{(x^*,u^*)} + \nabla_x g_1(x)u_1|_{(x^*,u^*)} + \nabla_x g_2(x)u_2|_{(x^*,u^*)} + \\ + \nabla_x g_3(x)u_3|_(x^*, u^*) + \nabla_x g_4(x)u_4|_{(x^*,u^*)} \end{aligned} \tag{32}$$

$$B = \nabla_u[f(x) + g(x)u]|_{(x^*,u^*)} \Rightarrow B = g(x)|_{(x^*,u^*)} \tag{33}$$

Next, the elements of the Jacobian matrix $\nabla_x f(x)|_{(x^*,u^*)}$ are computed:

First row of the Jacobian matrix $\nabla_x f(x)|_{(x^*,u^*)}$: $\frac{\partial f_1}{\partial x_1} = 0$, $\frac{\partial f_1}{\partial x_2} = 1$, $\frac{\partial f_1}{\partial x_3} = 0$, $\frac{\partial f_1}{\partial x_4} = 0$, $\frac{\partial f_1}{\partial x_5} = 0$ and $\frac{\partial f_1}{\partial x_6} = 0$.

Second row of the Jacobian matrix $\nabla_x f(x)|_{(x^*,u^*)}$: $\frac{\partial f_2}{\partial x_1} = 0$, $\frac{\partial f_2}{\partial x_2} = \left[\frac{B_{vn}}{M} sin^2(x_5) - \frac{B_v}{M} cos^2(x_5)\right]$, $\frac{\partial f_2}{\partial x_3} = 0$, $\frac{\partial f_2}{\partial x_4} = \left[-\left(\frac{B_v}{M} + \frac{B_{vn}}{M}\right) sin(x_5)cos(x_5)\right] - x_6$, $\frac{\partial f_2}{\partial x_5} = \left[2\frac{B_{vn}}{M} sin(x_5)cos(x_5) + 2\frac{B_v}{M} sin(x_5)cos(x_5)\right]x_2 + \left[-\left(\frac{B_v}{M} + \frac{B_{vn}}{M}\right)(cos^2(x_5) - sin^2\right.$ $(x_5))]x_4 + \frac{C_v}{M} sin(x_5)sign(cos(x_5)x_2 + sin(x_5)x_4) - \frac{C_{vn}}{M} cos(x_5)sign(-sin(x_5)x_2 + cos$ $(x_5)x_4)$, $\frac{\partial f_2}{\partial x_6} = -x_4$.

Third row of the Jacobian matrix $\nabla_x f(x)|_{(x^*,u^*)}$: $\frac{\partial f_3}{\partial x_1} = 0$, $\frac{\partial f_3}{\partial x_2} = 0$, $\frac{\partial f_3}{\partial x_3} = 0$, $\frac{\partial f_3}{\partial x_4} = 1$, $\frac{\partial f_3}{\partial x_5} = 0$ and $\frac{\partial f_3}{\partial x_6} = 0$.

Fourth row of the Jacobian matrix $\nabla_x f(x)|_{(x^*,u^*)}$: $\frac{\partial f_4}{\partial x_1} = 0$, $\frac{\partial f_4}{\partial x_2} = \left[\left(\frac{B_{vn}}{M} - \frac{B_v}{M}\right) sin(x_5)cos(x_5)\right] - x_6$, $\frac{\partial f_4}{\partial x_3} = 0$, $\frac{\partial f_4}{\partial x_4} = \left[-\frac{B_v}{M} sin^2(x_3) - \frac{B_{vn}}{M} cos^2(x_5)\right]$,

$\frac{\partial f_4}{\partial x_5} = \left[\frac{(B_{vn})}{M} - \frac{B_v}{M}(cos^2(x_5) - sin^2(x_5))\right]x_2 - \left[-2\frac{B_v}{M}sin(x_5)cos(x_5) + 2\frac{B_{vn}}{M}sin(x_5),\right.$ $cos(x_5)]x_4 - \frac{C_v}{M}cos(x_5)sign(cos(x_5)x_2 + sin(x_5)x_4) - \frac{C_{vn}}{M}sin(x_5)sign(-sin(x_5)x_2 +$ $cos(x_5)x_4)\,\frac{\partial f_4}{\partial x_6} = -x_4 - \frac{C_v}{M}cos(x_5)sign(cos(x_5)x_2 + sin(x_5)x_4) - \frac{C_{vn}}{M}sin(x_5)sign$ $(-sin(x_5)x_2 + = -x_4.$

Fifth row of the Jacobian matrix $\nabla_x f(x)|_{(x^*,u^*)}$: $\frac{\partial f_5}{\partial x_1} = 0$, $\frac{\partial f_5}{\partial x_2} = 0$, $\frac{\partial f_5}{\partial x_3} = 0$, $\frac{\partial f_5}{\partial x_4} = 0$, $\frac{\partial f_5}{\partial x_5} = 0$ and $\frac{\partial f_5}{\partial x_6} = 1$.

Sixth row of the Jacobian matrix $\nabla_x f(x)|_{(x^*,u^*)}$: $\frac{\partial f_6}{\partial x_1} = 0$, $\frac{\partial f_6}{\partial x_2} = 0$, $\frac{\partial f_6}{\partial x_3} = 0$, $\frac{\partial f_6}{\partial x_4} = 0$, $\frac{\partial f_6}{\partial x_5} = 0$ and $\frac{\partial f_6}{\partial x_6} = -\frac{B_v}{J}$.

Additionally, the Jacobian matrix $\nabla_x g_1(x)u_1|_{(x^*,u^*)}$ is computed:

$$\nabla_x g_1(x)u_1|_{(x^*,u^*)} = \begin{pmatrix} 0 & 0 & 0 & 0 & 0 & 0 \\ 0 & 0 & 0 & 0 & -\frac{l}{Mr}cos(x_5)u_1 & 0 \\ 0 & 0 & 0 & 0 & 0 & 0 \\ 0 & 0 & 0 & 0 & -\frac{l}{Mr}sin(x_5)u_1 & 0 \\ 0 & 0 & 0 & 0 & 0 & 0 \\ 0 & 0 & 0 & 0 & 0 & 0 \end{pmatrix}\Big|_{(x^*,u^*)} \tag{34}$$

Furthermore, the Jacobian matrix $\nabla_x g_2(x)u_2|_{(x^*,u^*)}$ is computed:

$$\nabla_x g_2(x)u_2|_{(x^*,u^*)} = \begin{pmatrix} 0 & 0 & 0 & 0 & 0 & 0 \\ 0 & 0 & 0 & 0 & \frac{l}{Mr}sin(x_5)u_2 & 0 \\ 0 & 0 & 0 & 0 & 0 & 0 \\ 0 & 0 & 0 & 0 & -\frac{l}{Mr}cos(x_5)u_2 & 0 \\ 0 & 0 & 0 & 0 & 0 & 0 \\ 0 & 0 & 0 & 0 & 0 & 0 \end{pmatrix}\Big|_{(x^*,u^*)} \tag{35}$$

Moreover, the Jacobian matrix $\nabla_x g_3(x)u_3|_{(x^*,u^*)}$ is computed:

$$\nabla_x g_3(x)u_3|_{(x^*,u^*)} = \begin{pmatrix} 0 & 0 & 0 & 0 & 0 & 0 \\ 0 & 0 & 0 & 0 & -\frac{l}{Mr}cos(x_5)u_3 & 0 \\ 0 & 0 & 0 & 0 & 0 & 0 \\ 0 & 0 & 0 & 0 & \frac{l}{Mr}sin(x_5)u_3 & 0 \\ 0 & 0 & 0 & 0 & 0 & 0 \\ 0 & 0 & 0 & 0 & 0 & 0 \end{pmatrix}\Big|_{(x^*,u^*)} \tag{36}$$

Finally, the Jacobian matrix $\nabla_x g_4(x)u_4|_{(x^*,u^*)}$ is computed:

$$\nabla_x g_4(x)u_4|_{(x^*,u^*)} = \begin{pmatrix} 0 & 0 & 0 & 0 & 0 & 0 \\ 0 & 0 & 0 & 0 & -\frac{l}{Mr}cos(x_5)u_4 & 0 \\ 0 & 0 & 0 & 0 & 0 & 0 \\ 0 & 0 & 0 & 0 & -\frac{l}{Mr}cos(x_5)u_4 & 0 \\ 0 & 0 & 0 & 0 & 0 & 0 \\ 0 & 0 & 0 & 0 & 0 & 0 \end{pmatrix}\Big|_{(x^*,u^*)} \tag{37}$$

3.2 Stabilising feedback control

After linearisation around its current operating point, the model of the omnidirectional four-wheel robot is written as [1]

$$\dot{x} = Ax + Bu + d_1 \tag{38}$$

Parameter d_1 stands for the linearisation error in the omnidirectional four-wheel robot's model appearing previously in Equation (38). The reference setpoints for the omnidirectional four-wheel robot's state vector are denoted by $\mathbf{x_d} = [x_1^d, \cdots, x_6^d]$. Tracking of this trajectory is achieved after applying the control input u^*. At every time instant the control input u^* is assumed to differ from the control input u appearing in Equation (38) by an amount equal to Δu, that is $u^* = u + \Delta u$

$$\dot{x}_d = Ax_d + Bu^* + d_2 \tag{39}$$

The dynamics of the controlled system described in Equation (38) can be also written as

$$\dot{x} = Ax + Bu + Bu^* - Bu^* + d_1 \tag{40}$$

and by denoting $d_3 = -Bu^* + d_1$ as an aggregate disturbance term one obtains

$$\dot{x} = Ax + Bu + Bu^* + d_3 \tag{41}$$

By subtracting Equation (39) from Equation (41) one has

$$\dot{x} - \dot{x}_d = A(x - x_d) + Bu + d_3 - d_2 \tag{42}$$

By denoting the tracking error as $e = x - x_d$ and the aggregate disturbance term as $\tilde{d} = d_3 - d_2$, the tracking error dynamics becomes

$$\dot{e} = Ae + Bu + \tilde{d} \tag{43}$$

For the approximately linearised model of the system a stabilising feedback controller is developed. The controller has the form

$$u(t) = -Ke(t) \tag{44}$$

with $K = \frac{1}{r}B^TP$ where P is a positive definite symmetric matrix which is obtained from the solution of the Riccati Equation [1]

$$A^TP + PA + Q - P\left(\frac{2}{r}BB^T - \frac{1}{\rho^2}LL^T\right)P = 0 \tag{45}$$

where Q is a positive semi-definite symmetric matrix. The diagram of the considered control loop for the omnidirectional mobile robot is depicted in Figure 2.

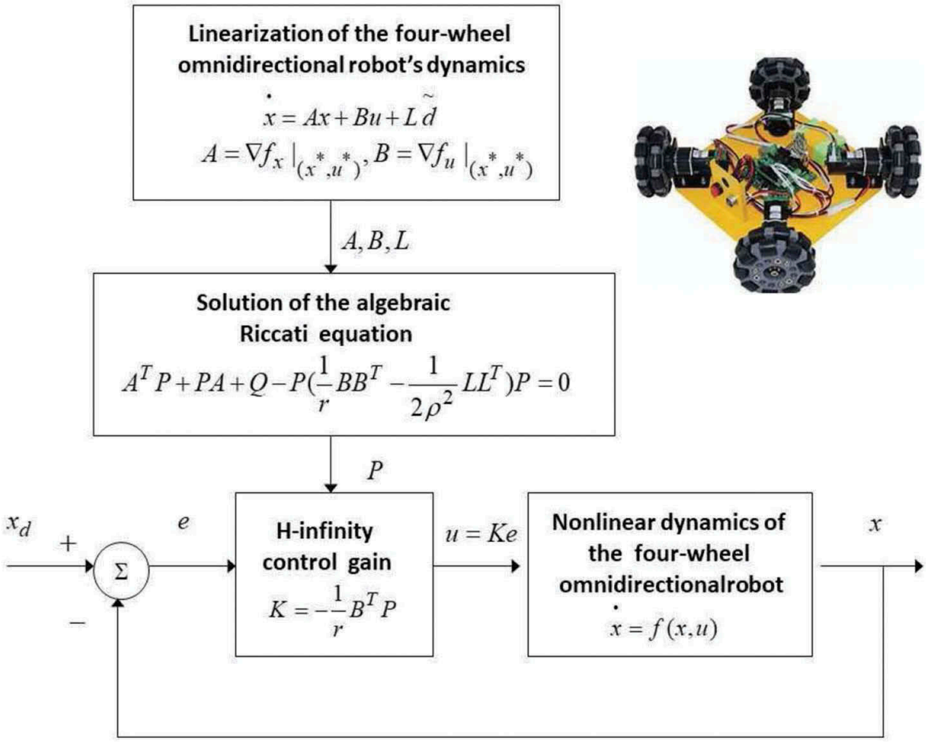

Figure 2. Diagram of the control scheme for the omnidirectional robot.

Remark 1: A comparison of the proposed non-linear optimal (H-infinity) control method against other linear and non-linear control schemes for omnidirectional four-wheel mobile robots, shows the following:

(1) unlike global linearisation-based control approaches, such as Lie algebra-based control and differential flatness theory-based control, the optimal control approach does not rely on complicated transformations (diffeomorphisms) of the system's state variables. Besides, the computed control inputs are applied directly on the initial non-linear model of the omnidirectional four-wheel ground vehicle and not on its linearised equivalent. The inverse transformations which are met in global linearisation-based control are avoided and consequently one does not come against the related singularity problems.

(2) unlike Model Predictive control (MPC) and Nonlinear Model Predictive control (NMPC), the proposed control method is of proven global stability. It is known that MPC is a linear control approach that if applied to the non-linear dynamics of the omnidirectional four-wheel ground vehicle the stability of the control loop will be lost. Besides, in NMPC the convergence of the iterative search for an optimum depends on initialisation

and parameter values selection and consequently the global stability of this control method cannot be always assured.

(3) unlike sliding mode control and backstepping control the proposed optimal control method does not require the state-space description of the system to be found in a specific form. About sliding-mode control it is known that when the controlled system is not found in the input-output linearised form the definition of the sliding surface can be an intuitive procedure. About backstepping control it is known that it can not be directly applied to a dynamical system if the related state-space model is not found in the triangular (backstepping integral) form.

(4) unlike PID control, the proposed non-linear optimal control method is of proven global stability, the selection of the controller's parameters does not rely on a heuristic tuning procedure, and the stability of the control loop is assured in the case of changes of operating points.

(5) unlike multiple local models-based control the non-linear optimal control method uses only one linearisation point and needs the solution of only one Riccati equation so as to compute the stabilising feedback gains of the controller. Consequently, in terms of computation load the proposed control method for the omnidirectional four-wheel ground vehicle's dynamics is much more efficient.

4 Lyapunov stability analysis

Through Lyapunov stability analysis it will be shown that the proposed non-linear control scheme assures H_∞ tracking performance for the overactuated omnidirectional robot, and that in case of bounded disturbance terms asymptotic convergence to the reference setpoints is succeeded. The tracking error dynamics for the omnidirectional mobile robot is written in the form

$$\dot{e} = Ae + Bu + L\tilde{d} \tag{46}$$

where in the omnidirectional robot's case $L = I \in R^6$ with I being the identity matrix. Variable $\tilde{d}$ denotes model uncertainties and external disturbances of the omnidirectional robot's model. The following Lyapunov equation is considered

$$V = \frac{1}{2}e^T P e \tag{47}$$

where $e = x - x_d$ is the tracking error. By differentiating with respect to time one obtains

$$\begin{aligned} \dot{V} &= \frac{1}{2}\dot{e}^T P e + \frac{1}{2}e^T P \dot{e} \Rightarrow \\ \dot{V} &= \frac{1}{2}[Ae + Bu + L\tilde{d}]^T P e + \frac{1}{2}e^T P[Ae + Bu + L\tilde{d}] \Rightarrow \end{aligned} \tag{48}$$

$$\dot{V} = \frac{1}{2}[e^T A^T + u^T B^T + \tilde{d}^T L^T]Pe + \\ + \frac{1}{2}e^T P[Ae + Bu + L\tilde{d}] \Rightarrow \tag{49}$$

$$\dot{V} = \frac{1}{2}e^T A^T Pe + \frac{1}{2}u^T B^T Pe + \frac{1}{2}\tilde{d}^T L^T Pe + \\ \frac{1}{2}e^T PAe + \frac{1}{2}e^T PBu + \frac{1}{2}e^T PL\tilde{d} \tag{50}$$

The previous equation is rewritten as

$$\dot{V} = \frac{1}{2}e^T(A^T P + PA)e + \left(\frac{1}{2}u^T B^T Pe + \frac{1}{2}e^T PBu\right) + \\ + \left(\frac{1}{2}\tilde{d}^T L^T Pe + \frac{1}{2}e^T PL\tilde{d}\right) \tag{51}$$

Assumption: For given positive definite matrix Q and coefficients r and ρ there exists a positive definite matrix P, which is the solution of the following matrix equation

$$A^T P + PA = -Q + P\left(\frac{2}{r}BB^T - \frac{1}{\rho^2}LL^T\right)P \tag{52}$$

Moreover, the following feedback control law is applied to the system

$$u = -\frac{1}{r}B^T Pe \tag{53}$$

By substituting Equation (52) and Equation (53) one obtains

$$\dot{V} = \frac{1}{2}e^T\left[-Q + P\left(\frac{2}{r}BB^T - \frac{1}{\rho^2}LL^T\right)P\right]e + \\ + e^T PB\left(-\frac{1}{r}B^T Pe\right) + e^T PL\tilde{d} \Rightarrow \tag{54}$$

$$\dot{V} = -\frac{1}{2}e^T Qe + \frac{1}{r}e^T PBB^T Pe - \frac{1}{2\rho^2}e^T PLL^T Pe \\ -\frac{1}{r}e^T PBB^T Pe + e^T PL\tilde{d} \tag{55}$$

which after intermediate operations gives

$$\dot{V} = -\frac{1}{2}e^T Qe - \frac{1}{2\rho^2}e^T PLL^T Pe + e^T PL\tilde{d} \tag{56}$$

or, equivalently

$$\dot{V} = -\frac{1}{2}e^T Q e - \frac{1}{2\rho^2}e^T PLL^T Pe + \\ +\frac{1}{2}e^T PL\tilde{d} + \frac{1}{2}\tilde{d}^T L^T Pe \tag{57}$$

Lemma: The following inequality holds

$$\frac{1}{2}e^T L\tilde{d} + \frac{1}{2}\tilde{d}L^T Pe - \frac{1}{2\rho^2}e^T PLL^T Pe \leq \frac{1}{2}\rho^2\tilde{d}^T\tilde{d} \tag{58}$$

Proof: The binomial $\left(\rho a - \frac{1}{\rho}b\right)^2$ is considered. Expanding the left part of the above inequality one gets

$$\rho^2 a^2 + \frac{1}{\rho^2}b^2 - 2ab \geq 0 \Rightarrow \frac{1}{2}\rho^2 a^2 + \frac{1}{2\rho^2}b^2 - ab \geq 0 \Rightarrow \\ ab - \frac{1}{2\rho^2}b^2 \leq \frac{1}{2}\rho^2 a^2 \Rightarrow \frac{1}{2}ab + \frac{1}{2}ab - \frac{1}{2\rho^2}b^2 \leq \frac{1}{2}\rho^2 a^2 \tag{59}$$

The following substitutions are carried out: $a = \tilde{d}$ and $b = e^T PL$ and the previous relation becomes

$$\frac{1}{2}\tilde{d}^T L^T Pe + \frac{1}{2}e^T PL\tilde{d} - \frac{1}{2\rho^2}e^T PLL^T Pe \leq \frac{1}{2}\rho^2\tilde{d}^T\tilde{d} \tag{60}$$

Equation (60) is substituted in Equation (57) and the inequality is enforced, thus giving

$$\dot{V} \leq -\frac{1}{2}e^T Q e + \frac{1}{2}\rho^2\tilde{d}^T\tilde{d} \tag{61}$$

Equation (61) shows that the H_∞ tracking performance criterion is satisfied. The integration of $\dot{V}$ from 0 to T gives

$$\int_0^T \dot{V}(t)dt \leq -\frac{1}{2}\int_0^T ||e||_Q^2 dt + \frac{1}{2}\rho^2\int_0^T ||\tilde{d}||^2 dt \Rightarrow \\ 2V(T) + \int_0^T ||e||_Q^2 dt \leq 2V(0) + \rho^2\int_0^T ||\tilde{d}||^2 dt \tag{62}$$

Moreover, if there exists a positive constant $M_d > 0$ such that $\int_0^\infty ||\tilde{d}||^2 dt \leq M_d$, then one gets

$$\int_0^\infty ||e||_Q^2 dt \leq 2V(0) + \rho^2 M_d \tag{63}$$

Thus, the integral $\int_0^\infty ||e||_Q^2 dt$ is bounded. Moreover, $V(T)$ is bounded and from the definition of the Lyapunov function V in Equation (47) it becomes clear that $e(t)$ will be also bounded since $e(t) \in \Omega_e = \{e | e^T Pe \leq 2V(0) + \rho^2 M_d\}$.

According to the above and with the use of Barbalat's Lemma one obtains $\lim_{t\to\infty} e(t) = 0$.

The outline of the global stability proof is that at each iteration of the control algorithm the state vector of the omnidirectional robot converges towards the temporary equilibrium and the temporary equilibrium in turn converges towards the reference trajectory. Thus, the control scheme exhibits global asymptotic stability properties and not local stability. Assume the *i*th iteration of the control algorithm and the *i*th time interval about which a positive definite symmetric matrix P is obtained from the solution of the Riccati Equation appearing in Equation (52). By following the stages of the stability proof one arrives at Equation (61) which shows that the H-infinity tracking performance criterion holds. By selecting the attenuation coefficient ρ to be sufficiently small and in particular to satisfy $\rho^2 < ||e||_Q^2/||\tilde{d}||^2$ one has that the first derivative of the Lyapunov function is upper bounded by 0. Therefore for the *i*th time interval it is proven that the Lyapunov function defined in Equation (47) is a decreasing one. This signifies that between the beginning and the end of the *i*th time interval there will be a drop of the value of the Lyapunov function and since matrix P is a positive definite one, the only way for this to happen is the Euclidean norm of the state vector error e to be decreasing. This means that comparing to the beginning of each time interval, the distance of the state vector error from 0 at the end of the time interval has diminished. Consequently as the iterations of the control algorithm advance the tracking error will approach zero, and this is a global asymptotic stability condition.

5 Robust state estimation with the use of the H_∞ Kalman Filter

The control loop has to be implemented with the use of information provided by a small number of sensors and by processing only a small number of state variables. To reconstruct the missing information about the state vector of the omnidirectional robot it is proposed to use a filtering scheme and based on it to apply state estimation-based control [35]. The recursion of the H_∞ Kalman Filter, for the model of the omnidirectional robot, can be formulated in terms of a *measurement update* and a *time update* part

Measurement update:

$$\begin{aligned} D(k) &= [I - \theta W(k)P^-(k) + C^T(k)R(k)^{-1}C(k)P^-(k)]^{-1} \\ K(k) &= P^-(k)D(k)C^T(k)R(k)^{-1} \\ \hat{x}(k) &= \hat{x}^-(k) + K(k)[y(k) - C\hat{x}^-(k)] \end{aligned} \tag{64}$$

Time update:

$$\begin{aligned} \hat{x}^-(k+1) &= A(k)x(k) + B(k)u(k) \\ P^-(k+1) &= A(k)P^-(k)D(k)A^T(k) + Q(k) \end{aligned} \tag{65}$$

where it is assumed that parameter θ is sufficiently small to assure that the covariance matrix $P^{-}(k)^{-1} - \theta W(k) + C^T(k)R(k)^{-1}C(k)$ will be positive definite. When $\theta = 0$ the H_∞ Kalman Filter becomes equivalent to the standard Kalman Filter. One can measure only a part of the state vector of the omnidirectional robot, for instance state variables x_1 (x-axis position of the omnidirectional robot), x_3 (y-axis position of the omnidirectional robot), and $x_5 = \theta$ (heading angle of the vehicle) and can estimate through filtering the rest of the state vector elements. Moreover, the proposed Kalman filtering method can be used for sensor fusion purposes.

6 Simulation tests

The performance of the proposed non-linear optimal (H-infinity) control scheme for the model of the omnidirectional mobile robot has been tested through simulation experiments. It is shown that under the proposed control method the mobile robot can truck accurately any reference trajectory. The convergence to the reference setpoints is fast, while the variations of the control inputs were moderate. The real values of the state variables of the mobile robot are plotted in blue, the estimated values are printed in green while the related reference setpoints are depicted in red. The tracking of the reference trajectories in the xy plane by the centre of gravity of the omnidirectional robot is shown in Figure 3 to Figure 5. Moreover, results about the convergence of the state variables to the reference setpoints and about the

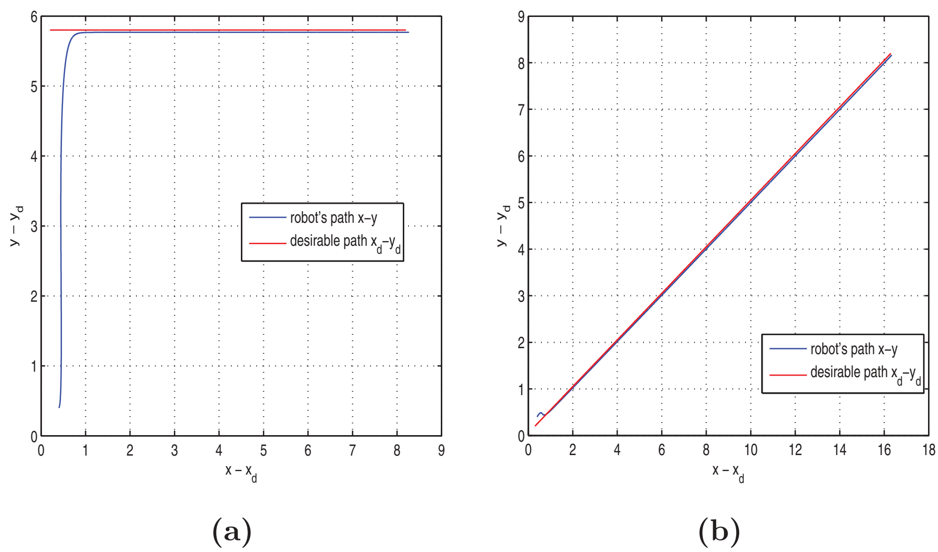

Figure 3. (a) Tracking of reference trajectory 1 on the xy plane (red line) by the centre of gravity (x, y) of the omnidirectional mobile robot (blue line). (b) Tracking of reference trajectory 2 on the xy plane (red line) by the centre of gravity (x, y) of the omnidirectional mobile robot (blue line).

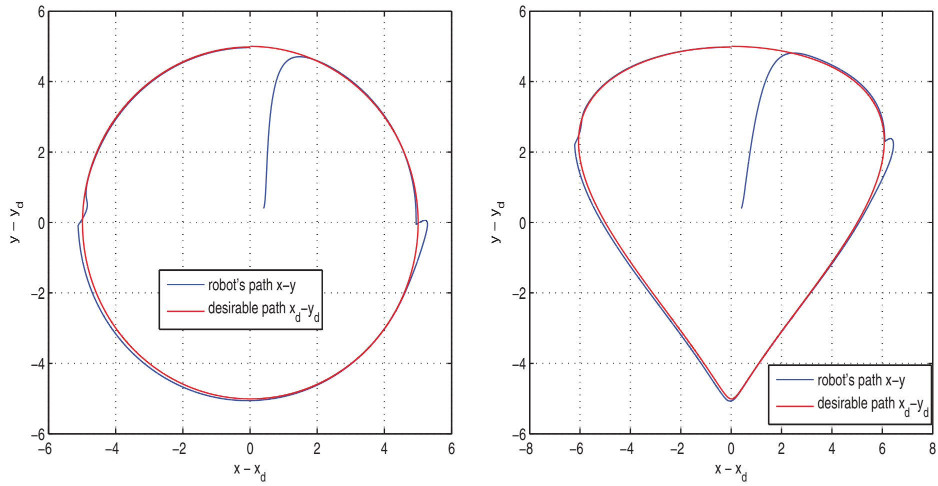

(a) (b)

Figure 4. (a) Tracking of reference trajectory 3 on the *xy* plane (red line) by the centre of gravity (x, y) of the omnidirectional mobile robot (blue line). (b) Tracking of reference trajectory 4 on the *xy* plane (red line) by the centre of gravity (x, y) of the omnidirectional mobile robot (blue line).

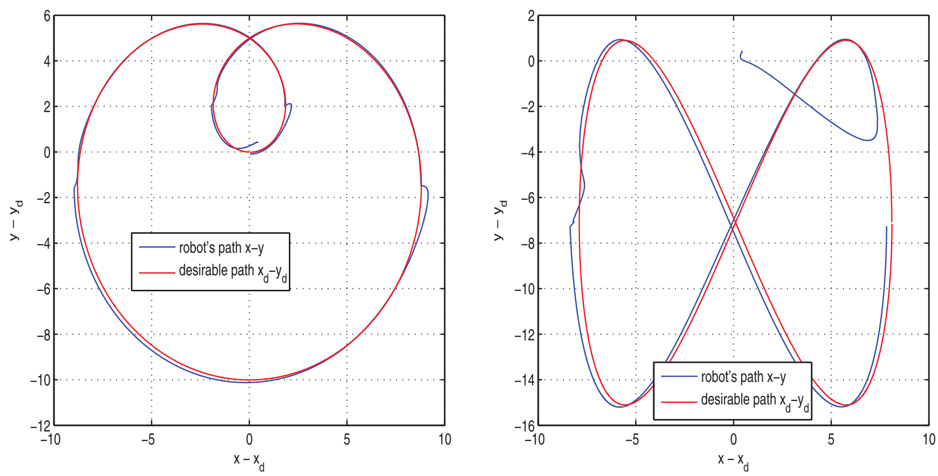

(a) (b)

Figure 5. (a) Tracking of reference trajectory 5 on the *xy* plane (red line) by the centre of gravity (x, y) of the omnidirectional mobile robot (blue line). (b) Tracking of reference trajectory 6 on the *xy* plane (red line) by the centre of gravity (x, y) of the omnidirectional mobile robot (blue line).

variation of the control inputs are depicted in Figures 6–12. To implement state estimation-based control there was need to measure only three of the state variables of the omnidirectional mobile robot, that is the position of the

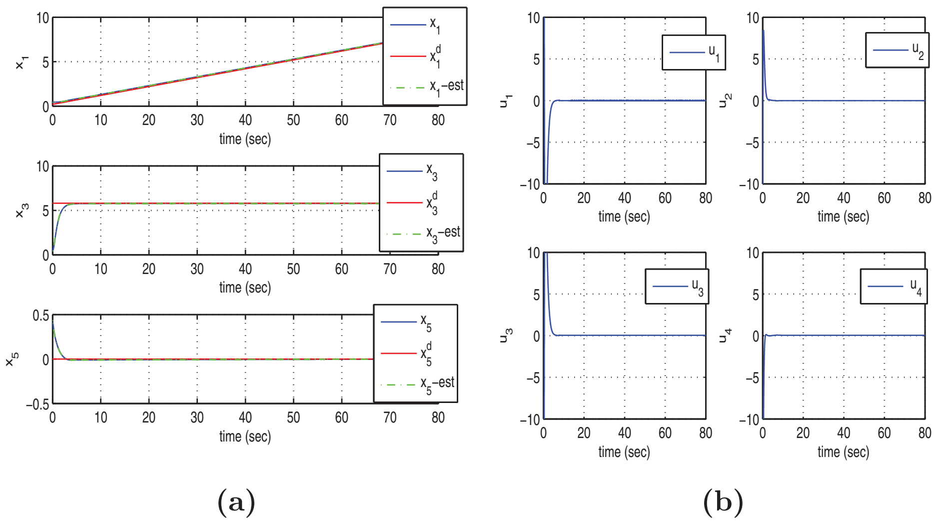

Figure 6. Tracking of setpoint 1 for the omnidirectional mobile robot (a) convergence of the state variables of the robot x_i, $i = 1, 3, 5$ to their reference setpoints (red line: setpoint, blue line: real value, green line: estimated value), and (b) control inputs u_i $i = 1, \cdots, 4$ applied to the mobile robot.

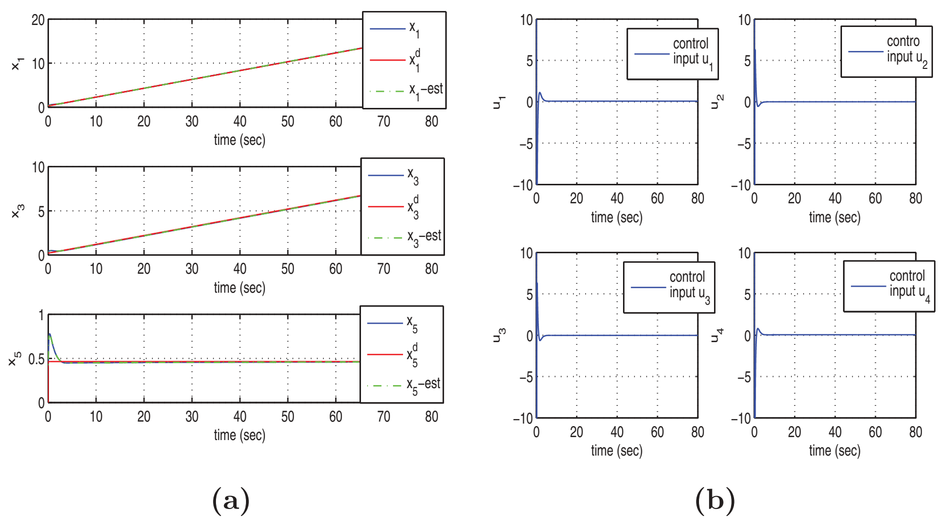

Figure 7. Tracking of setpoint 2 for the omnidirectional mobile robot (a) convergence of the state variables of the robot x_i, $i = 1, 3, 5$ to their reference setpoints (red line: setpoint, blue line: real value, green line: estimated value), and (b) control inputs u_i $i = 1, \cdots, 4$ applied to the mobile robot.

robot's centre of gravity on the x-axis that is $x_1 = x$, the position of the robot on the y-axis that is $x_3 = y$, and finally the heading angle of the robot $x_5 = \theta$.

The transient performance of the control scheme relies on the selection of specific parameters of the associated Riccati equation given in Equation (52).

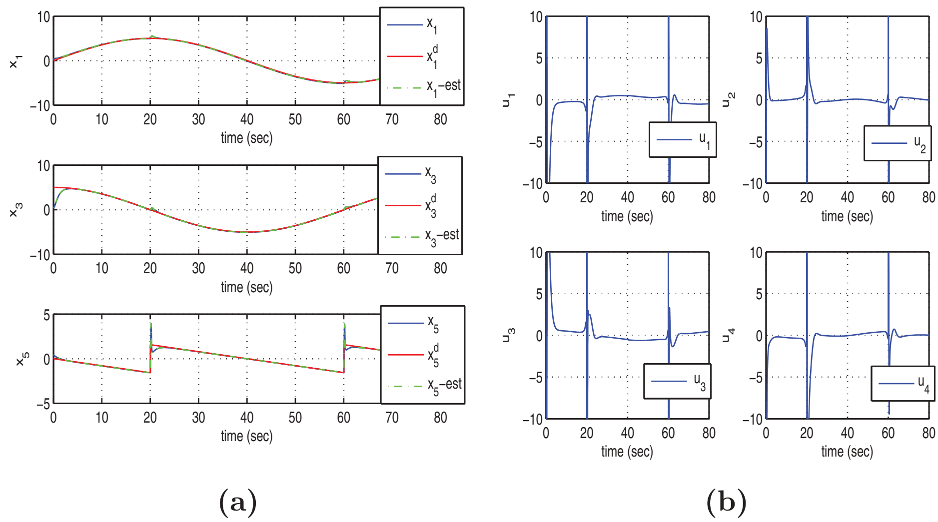

Figure 8. Tracking of setpoint 3 for the omnidirectional mobile robot (a) convergence of the state variables of the robot x_i, $i = 1, 3, 5$ to their reference setpoints (red line: setpoint, blue line: real value, green line: estimated value), and (b) control inputs u_i $i = 1, \cdots, 4$ applied to the mobile robot.

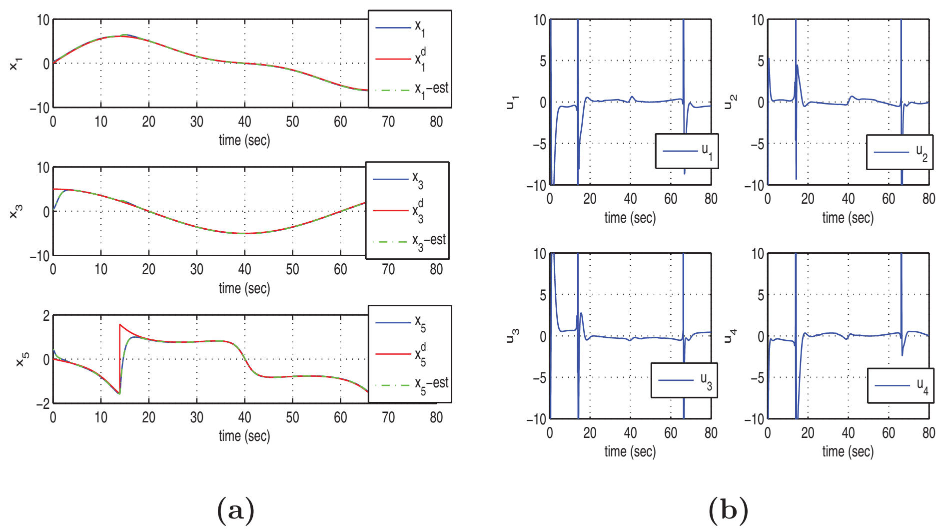

Figure 9. Tracking of setpoint 4 for the omnidirectional mobile robot (a) convergence of the state variables of the robot x_i, $i = 1, 3, 5$ to their reference setpoints (red line: setpoint, blue line: real value, green line: estimated value), and (b) control inputs u_i $i = 1, \cdots, 4$ applied to the mobile robot.

Such parameters are the gain r, the attenuation coefficient ρ and the weight matrix Q. The smallest value of ρ for which the Riccati equation admits as solution a positive definite matrix P is the one that provides the control loop with maximum robustness. The proposed control method retains the

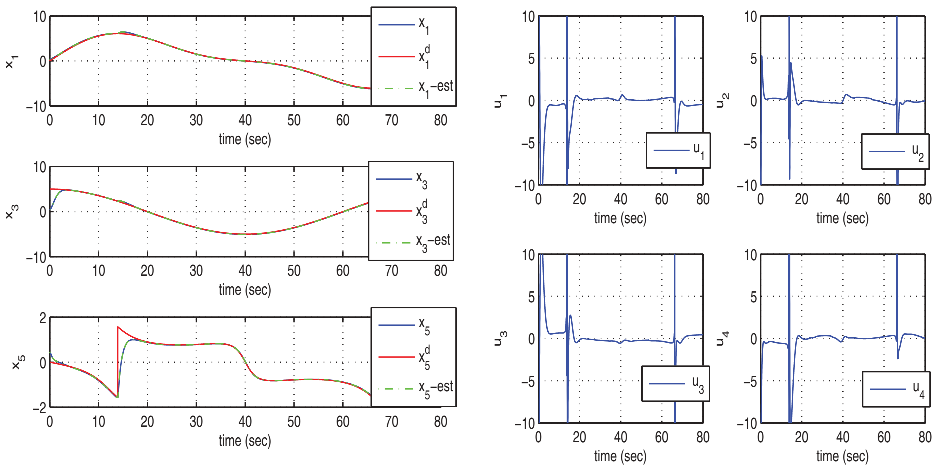

(a) (b)

Figure 10. Tracking of setpoint 4 for the omnidirectional mobile robot (a) convergence of the state variables of the robot x_i, $i = 1, 3, 5$ to their reference setpoints (red line: setpoint, blue line: real value, green line: estimated value), and (b) control inputs u_i $i = 1, \cdots, 4$ applied to the mobile robot.

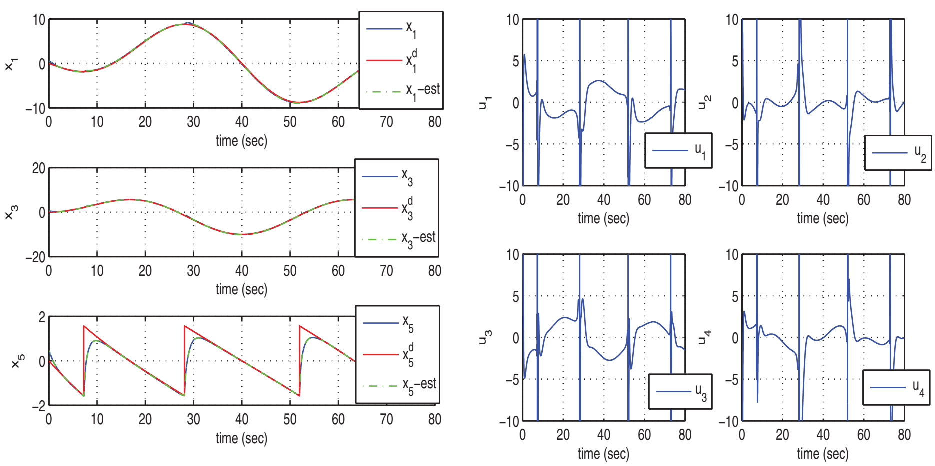

(a) (b)

Figure 11. Tracking of setpoint 5 for the omnidirectional mobile robot (a) convergence of the state variables of the robot x_i, $i = 1, 3, 5$ to their reference setpoints (red line: setpoint, blue line: real value, green line: estimated value), and (b) control inputs u_i $i = 1, \cdots, 4$ applied to the mobile robot.

advantages of optimal control such as: (i) there is fast and accurate tracking of the reference setpoints under moderate variations of the control inputs, (ii) the control inputs are applied directly on the non-linear model of the mobile robot and not on a linearised equivalent description of it (iii) unlike global linearisation

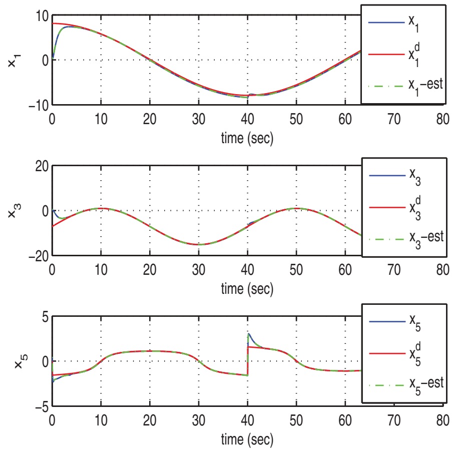

(a)

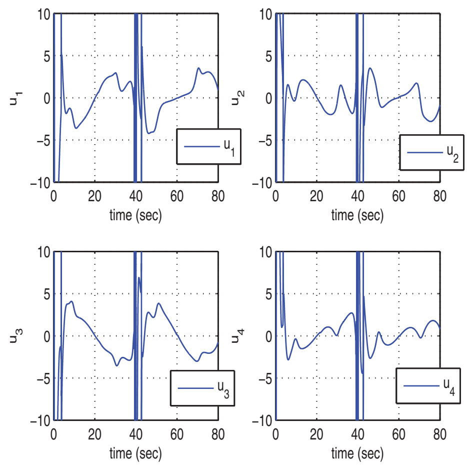

(b)

Figure 12. Tracking of setpoint 6 for the omnidirectional mobile robot (a) convergence of the state variables of the robot x_i, $i = 1, 3, 5$ to their reference setpoints (red line: setpoint, blue line: real value, green line: estimated value), and (b) control inputs u_i $i = 1, \cdots, 4$ applied to the mobile robot.

methods to compute the control input of the robot there is no need to perform inverse transformations and thus the risk for singularities is avoided.

Representative results about the tracking accuracy of the state variables of the omnidirectional four-wheel mobile robot under the non-linear optimal control method are given in Table 1. Moreover results about the robustness of the control method under parametric changes, for instance a change of $\Delta B_w\%$ of the viscous friction B_w from its nominal value, are given in Table 2. Furthermore, results about the estimation accuracy of the H-infinity Kalman Filter, for all state variables of the omnidirectional four-wheel mobile robot, are given in Table 3.

Remark 2: The theoretical contribution of this article is that it presents the only convergent and of assured performance solution to the non-linear optimal control problem of the omnidirectional four-wheel ground vehicle. Attempts to solve this non-linear optimal control problem with the use of MPC and NMPC have not been equally effective, since the stability properties of the related

Table 1. RMSE of the omnidirectional robot's state variables.

path	RMSE x_1	RMSE x_2	RMSE x_3	RMSE x_4	RMSE x_5	RMSE x_6
1	$2.8 \cdot 10^{-3}$	$0.1 \cdot 10^{-3}$	$1.6 \cdot 10^{-3}$	$0.1 \cdot 10^{-3}$	$0.1 \cdot 10^{-3}$	$0.1 \cdot 10^{-3}$
2	$1.8 \cdot 10^{-3}$	$0.1 \cdot 10^{-3}$	$1.9 \cdot 10^{-3}$	$0.1 \cdot 10^{-3}$	$0.2 \cdot 10^{-3}$	$0.1 \cdot 10^{-3}$
3	$2.1 \cdot 10^{-3}$	$0.1 \cdot 10^{-3}$	$1.1 \cdot 10^{-3}$	$0.1 \cdot 10^{-3}$	$0.1 \cdot 10^{-3}$	$0.1 \cdot 10^{-3}$
4	$1.2 \cdot 10^{-3}$	$0.1 \cdot 10^{-3}$	$1.1 \cdot 10^{-3}$	$0.1 \cdot 10^{-3}$	$0.2 \cdot 10^{-3}$	$0.1 \cdot 10^{-3}$
5	$8.5 \cdot 10^{-3}$	$0.6 \cdot 10^{-3}$	$1.1 \cdot 10^{-3}$	$0.6 \cdot 10^{-3}$	$0.7 \cdot 10^{-3}$	$0.3 \cdot 10^{-3}$
6	$6.5 \cdot 10^{-3}$	$0.1 \cdot 10^{-3}$	$3.3 \cdot 10^{-3}$	$0.1 \cdot 10^{-3}$	$1.3 \cdot 10^{-3}$	$0.1 \cdot 10^{-3}$

Table 2. RMSE of the omnidirectional robot under disturbances.

$\Delta B_w\%$	RMSE x_1	RMSE x_2	RMSE x_3	RMSE x_4	RMSE x_5	RMSE x_6
0%	$2.1 \cdot 10^{-3}$	$0.1 \cdot 10^{-3}$	$1.1 \cdot 10^{-3}$	$0.1 \cdot 10^{-3}$	$0.1 \cdot 10^{-3}$	$0.1 \cdot 10^{-3}$
10%	$2.6 \cdot 10^{-3}$	$0.1 \cdot 10^{-3}$	$1.2 \cdot 10^{-3}$	$0.1 \cdot 10^{-3}$	$0.1 \cdot 10^{-3}$	$0.1 \cdot 10^{-3}$
20%	$2.8 \cdot 10^{-3}$	$0.1 \cdot 10^{-3}$	$1.2 \cdot 10^{-3}$	$0.1 \cdot 10^{-3}$	$0.1 \cdot 10^{-3}$	$0.1 \cdot 10^{-3}$
30%	$3.2 \cdot 10^{-3}$	$0.1 \cdot 10^{-3}$	$1.2 \cdot 10^{-3}$	$0.1 \cdot 10^{-3}$	$0.1 \cdot 10^{-3}$	$0.1 \cdot 10^{-3}$
40%	$3.7 \cdot 10^{-3}$	$0.1 \cdot 10^{-3}$	$1.2 \cdot 10^{-3}$	$0.1 \cdot 10^{-3}$	$0.2 \cdot 10^{-3}$	$0.1 \cdot 10^{-3}$
50%	$3.9 \cdot 10^{-3}$	$0.1 \cdot 10^{-3}$	$1.2 \cdot 10^{-3}$	$0.1 \cdot 10^{-3}$	$0.2 \cdot 10^{-3}$	$0.1 \cdot 10^{-3}$
60%	$4.0 \cdot 10^{-3}$	$0.1 \cdot 10^{-3}$	$1.2 \cdot 10^{-3}$	$0.1 \cdot 10^{-3}$	$0.2 \cdot 10^{-3}$	$0.1 \cdot 10^{-3}$

Table 3. RMSE of state estimation with the H-infinity KF.

path	RMSE x_1	RMSE x_2	RMSE x_3	RMSE x_4	RMSE x_5	RMSE x_6
1	$2.6 \cdot 10^{-3}$	$0.1 \cdot 10^{-3}$	$1.6 \cdot 10^{-3}$	$0.1 \cdot 10^{-3}$	$0.1 \cdot 10^{-3}$	$0.1 \cdot 10^{-3}$
2	$1.8 \cdot 10^{-3}$	$0.1 \cdot 10^{-3}$	$1.9 \cdot 10^{-3}$	$0.1 \cdot 10^{-5}$	$0.2 \cdot 10^{-3}$	$0.1 \cdot 10^{-3}$
3	$2.1 \cdot 10^{-3}$	$0.1 \cdot 10^{-3}$	$1.2 \cdot 10^{-3}$	$0.1 \cdot 10^{-3}$	$0.1 \cdot 10^{-3}$	$0.1 \cdot 10^{-3}$
4	$1.7 \cdot 10^{-3}$	$0.1 \cdot 10^{-3}$	$1.0 \cdot 10^{-3}$	$0.1 \cdot 10^{-3}$	$0.1 \cdot 10^{-3}$	$0.1 \cdot 10^{-3}$
5	$3.3 \cdot 10^{-3}$	$0.3 \cdot 10^{-3}$	$2.5 \cdot 10^{-3}$	$0.1 \cdot 10^{-3}$	$0.4 \cdot 10^{-3}$	$0.1 \cdot 10^{-3}$
6	$6.4 \cdot 10^{-3}$	$0.1 \cdot 10^{-3}$	$3.3 \cdot 10^{-3}$	$0.4 \cdot 10^{-3}$	$1.4 \cdot 10^{-3}$	$0.1 \cdot 10^{-3}$

control loops and the convergence of these control algorithms to an optimum is other doubtful. The practical contribution of the article is that it introduces a control method which achieves accurate tracking of the desirable paths for the robot under moderate variations of the control inputs. By avoiding excessive values of the control inputs, the proposed method makes less frequent the need for batteries recharging, thus improving the operational capacity and prolonging the autonomous functioning of this specific type of mobile robots.

Remark 3: The proposed control method has been already applied with success to various models of autonomous robotic vehicles. The results of the present article show that the method has an excellent performance also in the case of the omnidirectional four-wheel mobile robot. As noted above, the proposed non-linear optimal control method exhibits several advantages when compared to other non-linear control methods for the model of the omnidirectional four-wheel autonomous ground vehicle. These advantages can be outlined once again as follows: (i) it avoids the complicated state space transformations and the singularity problems which can be met in global linearisation-based control schemes, (ii) it is of proven global stability and convergence to an optimum. (iii) it performs well in varying operating conditions of the robotic vehicle, (iv) it is computationally efficient, and (v) it is energy efficient thus improving the operational capacity of the mobile robot.

7 Conclusions

A non-linear optimal (H-infinity) control method has been introduced for the dynamic model of the four-wheel omnidirectional mobile robot. The method compensates for the non-linearities and multivariable structure of this mobile robot and despite overactuation it achieves optimal (energy efficient) computation of the vehicle's control inputs. To implement this control scheme, the dynamic model of the robot has undergone first approximate linearisation around a temporary operating point which was recomputed at each time-step of the control method. The linearisation procedure relied on Taylor series expansion and on the computation of the associated Jacobian matrices. The H-infinity control scheme represents a min-max differential game in which the controller tries to minimise a quadratic cost function of the state vector's tracking error whereas the modelling imprecision and exogenous perturbation terms try to maximise this cost function.

To compute the feedback gains of the H-infinity controller, an algebraic Riccati equation had to be repetitively solved at each time-step of the control method. The stability properties of the control method were proven through Lyapunov analysis. First, it was shown that the control scheme satisfies the H-infinity tracking performance criterion which signifies elevated robustness against modelling uncertainty and external perturbations. Next, it was shown that the control loop is also globally asymptotically stable, which signifies elimination of the tracking error for the state variables of the system. Finally, to implement state estimation-based control without the need to measure the complete state vector of the system, the H-infinity Kalman Filter has been introduced as a robust state estimator.

Disclosure statement

No potential conflict of interest was reported by the authors.

Funding

This work was supported by the Unit of Industrial Automation/Industrial Systems Institute Ref 6065/Advances in Applied Nonlinear Optimal Control.

ORCID

G. Rigatos http://orcid.org/0000-0002-2972-7030

References

[1] Rigatos G, Busawon K. Robotic manipulators and vehicle: control, estimation and filtering. Cham. Switzerland: Springer; 2018.

[2] Huang JT, Hung TN, Tseng ML. Smooth switching robust adaptive control for omnidirectional mobile robots. IEEE Trans Control Syst Technol. 2015;23(5):1986–1993.

[3] Purwin O, D’ Andrea R. Trajectory generation and control for four wheeled omnidirectional vehicles. Rob Auton Syst. Elsevier. 2006;54:13–22.

[4] Konjanawanishkal K, Zelli A. A model-predictive approach to formation control of omnidirectional mobile robots, 2008. IEEE/RSJ International Conference o Intelligent Robots and Systems., Nice, France, Sep. 2008.

[5] Kim KB, Kim BK. Minimum-time trajectory for three-wheeled omnidirectional mobile robots following a bounded curvature with a referenced heading profile. IEEE Trans Rob. 2011;27(4):800–808.

[6] Rotondo D, Puig V, Nejjan F, et al. A fault-hiding approach for the switching quasi-LPV fault-tolerant control of a four-wheeled omnidirectional mobile robot. IEEE Trans Ind Electron. 2015;62(6.):3932–3945.

[7] Huang HC, Tsai CC. FPGA implementation of an embedded robust adaptive controller for autonomous omnidirectional mobile platform. IEEE Trans Ind Electron. 2009;56 (5):1604–1616.

[8] Huang HC. SoPC-based parallel ACO algorithm and its application to optimal motion controller design for intelligent omnidirectional mobile robots. IEEE Trans Ind Inform. 2013;9(4):1828–1836.

[9] Xu D, Zhao D, Yi J, et al. Trajectory tracking control of omnidirectional wheeled mobile manipulators: robust neural network-based sliding-mode approach. IEEE Trans Syst Man Cybern Syst. 2009;39(3):788–799.

[10] Scolari-Conceicao A, Moreira AP, Costa PJ. A nonlinear model predictive control strategy for trajectory tracking of a four-wheeled omnidirectional mobile robot, optimal control applications and Methods. J Wiley. 2008;29:352–395.

[11] Sprunk C, Lau B, Pfaff P, et al. An accurate and efficient navigation system for omnidirectional robots in industrial environments. Auton Rob. Springer. 2017;41(2):473–493.

[12] Rotondo R, Nejjari F, Puig V. Model reference switching quasi-LPV control of a four wheeled omnidirectional robot. 19th IFAC World Congress; Aug; Cape Town, South Africa; 2014.

[13] Oliveira HP, Sousa AI, Moreira AP, et al. Modelling and assessing of omnidirectional robots with three and four wheels. Contemporary Robotics - Challenges and Solutions, A.D. Radi (Editor), InTech Open. doi:19.5772/7796. .

[14] Oliveira HP, Sousa AJ, Moreira AP, et al. Precise modelling of a four-wheeled omnidirectional robot. Proceedings Robotica Conference 2008, 8th Conference on Autonomous Robot Systems and Competitions, University of Aveiro Portugal, April 2008.

[15] Vasquez JA, Veloso-Villa M. Path-tracking dynamic model-based control of an omnidirectional mobile robot. Proceedings 17th IFAC World Congress; Jul; Seoul, South Korea; 2008.

[16] Huang N, Viet TD, Im JS, et al. Motion control of an omnidirectional mobile platform trajectory tracking using an integral sliding-mode controller, Intl. Journal of Control. Autom Sys. Springer. 2010;8(6):1221–1231.

[17] Zhao D, Deng X, Yi J. Motion and internal force control for omnidirectional wheeled mobile robots. IEEE Trans Mechatron. 2009;14(3):382–387.

[18] Clavien L, Lauria M, Michaud F. Instantaneous center of rotation=based motion control for omnidirectional mobile robots with sidewards off-centered wheels. Rob Auton Syst. Elsevier. 2018;106:58–68.

[19] Song JB, Kim JK. Energy efficient drive of an omnidirectional mobile robot with steerable omnidirectional wheels. 16th Triennial IFAC World Congress; Prague, Czech Republic; 2005.

[20] Bourgein F, Desbiens A. Nonlinear multivariable control of an omnidirectional vehicle. 16th IFAC World Congress; Prague, Czech Republic; 2005.

[21] Scolari Conceicao A, Oliveira HR. Sousa de Silva A, et al. A nonlinear model predictive control of an omnidirectional mobile robot, IEEE Conf: Intl. Symposium on Industrial Electronics, Vigo, Spain; 2007.

[22] Jianbin W, Jianping C. An adaptive sliding-mode controller for four-wheeled omnidirectional mobile robot with input constraints. IEEE CCC 2019, IEEE 2019 Chinese Control Conference. June; Nanchang, China; 2019.

[23] Yang T, Sun N, Chen H, et al. Neural network-based adaptive antiswing control of an underactuated ship-mounted crane with roll motion and input dead zones. IEEE Transactions on Neural Networks and Learning Systems; 2019. doi:10.1109/TNNLS.2019.2910580.

[24] Wang J, Chen J, Xiao Q. A minimum-energy trajectory tracking controller for four-wheeled omnidirectional mobile robots. IEEE ICARCV 2018, IEEE 2018 15th Intl. Conf. on Control, Automation, Robotics and Vision; Nov; Singapore; 2018.

[25] Ferro M, Paolillo A, Cherubini A, et al. Vision-based navigation of omnidirectional mobile robots. IEEE Rob Autom Lett. 2019;4(3):2691–2698.

[26] Wu Z, Karimi HR, Dong C. An approximate algorithm for graph partitioning via deterministing annealing neural network. Neural Networks. Elsevier. 2019;117:191–200.

[27] Wu Z, Jian B, Cao Y. Finite-time H_∞ filtering for Ito stochastic Markovian jump systems with distributed time-varying delays based on optimization algorithm. IET Control Theory Appl. 2019;13(5):702–710.

[28] Sun N, Liang D, Wu Y, et al. Adaptive control for pneumatic artificial muscle systems with parametric uncertainties and unidirectional input constraints. IEEE Trans Ind Inform. 2019;16(2):969–979.

[29] Rigatos G. Intelligent Renewable Energy Systems: modelling and Control. Cham, Switzerland: Springer; 2016.

[30] Rigatos G, Siano P, Wira P, et al. Nonlinear H-infinity feedback control for asynchronous motors of electric trains. J Intell Indus Syst. Springer. 2015;1:85–98.

[31] Rigatos GG, Tzafestas SG. Extended Kalman filtering for fuzzy modelling and multi-sensor fusion. Math Comput Modell Dyn Syst. Taylor & Francis. 2007;13:251–266.

[32] Basseville M, Nikiforov I. Detection of abrupt changes: theory and applications. New Jersey (USA): Prentice-Hall; 1993.

[33] Rigatos G, Zhang Q. Fuzzy model validation using the local statistical approach. Fuzzy Sets Syst. Elsevier. 2009;60(7):882–904.

[34] Rigatos G. Modelling and control for intelligent industrial systems. In: adaptive algorithms in robotics and industrial engineering. Berlin-Heidelberg, Germany: Springer; 2011.

[35] Rigatos G. Nonlinear control and filtering using differential flatness theory approaches: applications to electromechanical systems. Cham, Switzerland: Soriner; 2015.

[36] Rigatos G, Siano P, Cecati C. A new non-linear h-infinity feedback control approach for three-phase voltage source converters. Electr Pow Compo Sys. Taylor and Francis. 2015;44(3):302–312.

[37] Toussaint GJ, Basar T, Bullo F, H_∞ optimal tracking control techniques for nonlinear underactuated systems. Proceedings IEEE CDC 2000, 39th IEEE Conference on Decision and Control; Sydney Australia; 2000.

[38] Lublin L, Athans M. An experimental comparison of H_2 and H_∞ designs for interferometer testbed, lectures notes in control and information sciences: feedback control, nonlinear systems and complexity. (Francis B. and Tannenbaum A., eds.). London: Springer; 1995. p. 150–172.

[39] Gibbs BP. Advanced Kalman filtering, least squares and modelling: A practical handbook. J Wiley. 2011.

[40] Simon D. A game theory approach to constrained minimax state estimation. IEEE Trans Signal Process. 2006;54(2):405–412.